Multi-physical analysis of the electrochemical behavior of OFHC copper surfaces obtained by orthogonal cutting

L.A. Denguir[a,b]*, J.C. Outeiro[a], G. Fromentin[a]

[a]*LaBoMaP, Arts et Métiers Institute of Technology, 71250 Cluny, FRANCE*
[b]*ICB UMR 6303 -Université de Bourgogne-Franche Comté, 21078 Dijon, France*

* Corresponding author e-*mail address*: lamice.denguir@knowledgeandskills.eu

ARTICLE INFO

Keywords:

Surface Integrity
Corrosion;
OFHC Copper;
Orthogonal Cutting;
Electrochemical behavior.

ABSTRACT

As mechanical, physical, and microstructural properties of metals can be significantly affected by the machining process, electrochemical properties and corrosion resistance are consequently altered. Manufacturers should control the impact of cutting conditions on surface integrity, as it will affect the component's functional performance and life. This study addresses the case of orthogonal cutting of oxygen-free high conductivity (OFHC) copper. A set of experiments was performed and a statistical analysis was conducted to reveal the relationship between the cutting conditions and the surface integrity in terms of residual stresses, microstructure, plastic deformation and hardness, and the impact of those parameters on the electrochemical behavior. The physical origins of the observed phenomena are explained. The results show that the surface performance can be controlled by selecting the appropriate cutting conditions (e.g., reducing the tensile residual stress and roughness by more than 75%), such that the electrochemical behavior can be enhanced.

GRAPHICAL ABSTRACT

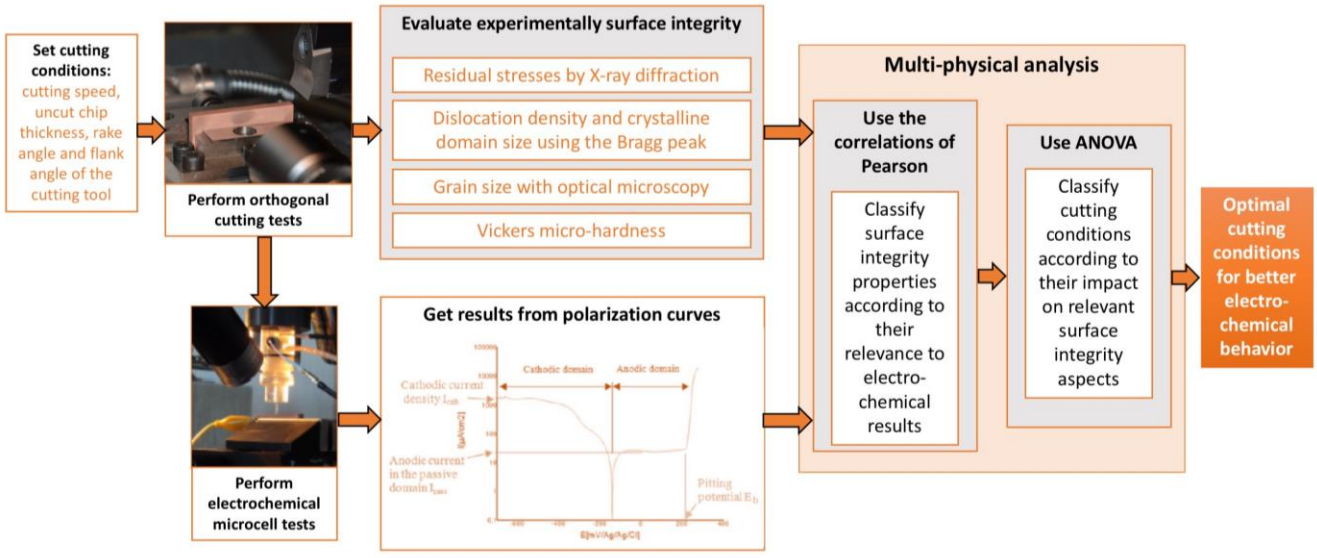

HIGHLIGHTS

- Performing orthogonal cutting tests varying cutting conditions on OFHC copper.
- Analyzing mechanical and microstructural state of OFHC copper machined surfaces including roughness, residual stresses, grain size and dislocation density.
- Analyzing the electrochemical behavior of the machined surfaces using polarization curves issued from electrochemical microcell tests.
- Relating surface integrity mechanical and microstructural properties to electrochemical properties using statistical analysis.
- Optimizing cutting conditions to control the surface integrity state and then ameliorate the corrosion resistance.

1. Introduction

Corrosion of copper and its alloys has been widely studied in chloride media, since it has been observed that the chloride ion has a strong influence on the copper corrosion mechanism [1]. As the mechanical, physical, and microstructural properties of metals can be significantly affected by the machining process [2], the electrochemical and corrosion resistance properties are consequently altered. In fact, owing to its functional and economical relevance, corrosion of metallic materials has been the focus of several investigations, especially as pitting and intergranular corrosion can present potential initiation sites for cracks, resulting in failure. To control the impact of corrosion on surface life and performance, some investigations explored the relationships between the parameters of surface integrity and the electrochemical reactivity and/or corrosion resistance of the materials in different environments.

In fact, several metals have been studied to address corrosion resistance at a microscopic scale. For example, in duplex stainless steels with both austenitic and ferritic structures, owing to the differences of mechanical properties in both phases in addition to their morphology, a heterogeneous distribution of strains is generated [3]. This gradient of strain can affect the physicochemical properties of the material [4]. Vignal and Kempf [5] performed local electrochemical measurements using an NaCl solution with an electrochemical microcell technique [6] on UNS S31803 duplex steel having a surface containing glide planes and microcracks. They proposed a mechanical-electrochemical criterion aiming to significantly enhance the anodic and/or the cathodic reaction while reducing the pitting of the deformed material. Another study led by Krawiec et al. [7] addressed local electrochemical behavior of the aluminum alloy $AlCu_4Mg_1$ containing large precipitates. They demonstrated that the most active sites are those that correspond to microcracks and other damage to the metal matrix. However, local polarization curves performed on sites containing precipitates, but free of defaults induced by the deformations, are too close to those obtained inside the grains far from the precipitates. To summarize, heterogeneity of the material as well as damage and microcracks due to deformations are shown in literature as the principle precursors of any change in the electrochemical behavior of metallic materials.

Concerning the electrochemical behavior of copper, which has a monophasic microstructure, other aspects of surface integrity must be considered while studying its local characteristics. It is then necessary to quantify the residual stresses, textures, and microstructure induced by the manufacturing process. In the investigation of Bissey-Breton et al. [8], which examined the case of the oxygen-free high conductivity (OFHC) copper-turning process, the influence of the nose radius of the cutting tool, the cutting velocity, and the lubricant on the residual stresses and the texture were evaluated. Next, the effects of these surface integrity parameters on electrochemical behavior were studied. Researchers determined that the stress gradient near the surface depends on the tool geometry and the depth of cut. Moreover, they determined that the smallest depth of cut with the presence of a lubricant leads to a higher anodic corrosion potential [8]. Later, Bissey-Breton et al. [9] found a relationship between surface

integrity parameters (in particular, the roughness and the residual stresses) and the free corrosion potential while testing the effect of the NaCl-aerated solution on the local electrochemical behavior of OFHC copper. Furthermore, to explain the observed impact of roughness on the local electrochemical behavior of copper, a theoretical demonstration has been performed by Li and Li [10] showing the noticeable rise in the Electron Work Function (*EWF*) fluctuation in the presence of peaks in the surface topography. In fact, such fluctuation can promote the formation of microelectrodes and consequently, accelerate corrosion. In addition, Yin and Li [11] determined that the initial grain size, the grain boundaries, and twins have an impact on the profile of subsurface residual stresses, which affects corrosive wear of copper surfaces when they are exposed to a saline solution of NaCl. In addition to the microstructure and the topography, sudden plastic deformation induced by the process has an impact on the electrochemical reactivity of the surface.

Although investigations in literature revealed some relations between the surface integrity of copper and its electrochemical reactivity in a saline environment, each one is still limited to the specific applications/processes that were tested and does not explicitly provide universal solutions to enhancing corrosion resistance with manufacturing process parameter choices. Indeed, the surface integrity induced by the turning process is different from the one obtained by orthogonal cutting owing to the fact that the cutting geometry induces different mechanical loadings and surface topography and consequently, the electrochemical behavior differs [12].

An understanding based on physical explanations should be assigned to the observed phenomena, from the manufacturing parameter choice to the control of the final surface reactivity inside its functional environment, through an analysis of the induced surface integrity. Following this reasoning, the present research focuses on the impact of the orthogonal cutting process on the local electrochemical reactivity of OFHC copper surfaces under saline solution. We provide practical recommendations for the choices of cutting conditions and cutting tool geometry, aiming to ameliorate the electrochemical behavior and consequently improve the surface performance and life of the metal.

The main focus of this study concerns the electrochemical characteristics of the copper metal/chloride corrosion system. First, a set of experiments is performed varying the cutting conditions including cutting speed and uncut chip thicknesses, as well as different tools geometries varying the rake angle and the flank angle. Then, surface integrity is evaluated in terms of residual stresses, microhardness, plastic layer thickness, surface roughness, grain size, and dislocations density. Finally, the electrochemical behavior of the different surfaces is evaluated using an electrochemical microcell technique. All results are analyzed using a multi-physical statistical analysis to reveal the surface integrity parameters ruling the electrochemical reactivity, as well as identify the cutting conditions causing those surface integrity states. Finally, the relationships between the prevailing parameters are

explained and the different observed phenomena are physically analyzed, revealing the optimal cutting conditions.

Nomenclature

d_{crys}	*Crystalline domain size in the crystallographic direction*
d_{grain}	*Grain size*
E_b	*Pitting potential*
EWF	*Electron work function*
eE_b	*Deviation corresponding to the measured parameter* E_b
eI_{cath}	*Deviation corresponding to the measured parameter* I_{cath}
eI_{pass}	*Deviation corresponding to the measured parameter* I_{pass}
F_i	*Fisher index*
FWHM	*Full width at half maximum*
h	*Uncut chip thickness*
HV	*Vickers microhardness*
I_{cath}	*Current density inside the cathodic domain*
I_{pass}	*Current density in the passive plate*
OFHC	*Oxygen free high conductivity*
r_n	*Edge radius*
r_{xy}	*Bravais-Pearson correlation coefficient*
S_a	*Surface arithmetic roughness*
S_t	*Surface roughness at maximum height*
V_c	*Cutting speed*
α	*Flank angle*
γ	*Rake angle*
ρ	*Dislocation density*
σ_x	*Residual stress at the surface measured in the cutting direction*
σ_y	*Residual stress at the surface measured in the transversal direction*

2. Experimental setup and methods

2.1. Orthogonal cutting tests

Orthogonal cutting tests were performed in the planing configuration (Figure 1) on flat specimens (40 x 15 x 4 mm) of OFHC copper (annealed at 450 °C for 2 hours, with an average grain size of 55 µm), using a DMG DMC85V milling machine. Uncoated cemented tungsten carbide cutting tools with four different geometries were used. All tool geometries were characterized by an edge radius (r_n) of 10 ± 2 µm. Rake angle values (γ) of 20° and 30° and flank angles (α) of 5° and 10° were used, and two uncut chip thickness (h) values of 0.05 and 0.2 mm were used. The cutting speeds (V_c) used were 90 and

120 m/min. The width of cut (*W*) was kept constant and equal to 4 mm. Low temperature pressurized air (−5 ± 2 °C; 6 bar) cooling generated by a vortex system was applied to minimize the adhesion phenomenon between the tool and the work material. The cutting parameters and tool geometry details are shown in Figure 1.

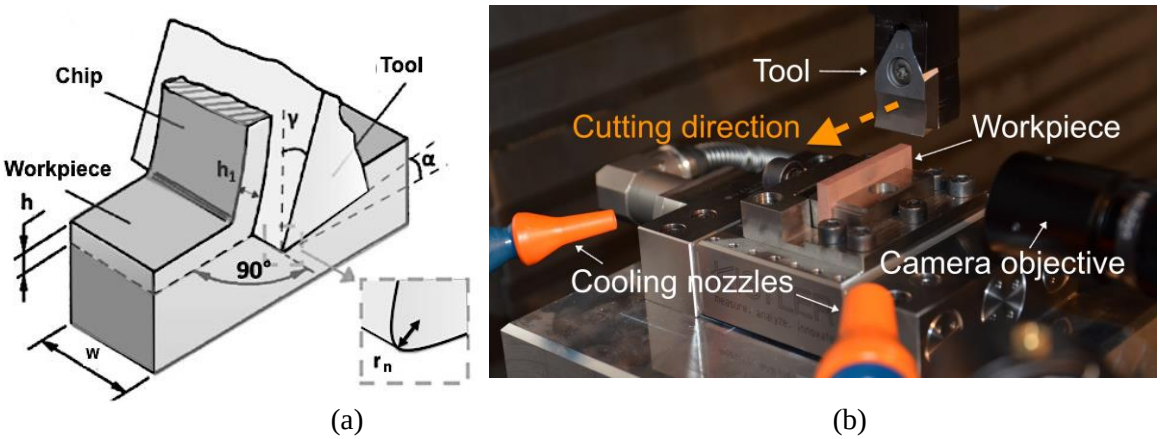

(a) (b)

Figure 1. *Orthogonal cutting: (a) geometry and parameters; (b) experimental setup.*

2.2. Mechanical and microstructural state analysis methods

Residual stresses were determined using a PROTO IXRD diffractometer, based on the X-ray diffraction technique, and by applying the $\sin^2\psi$ method. According to this method, the residual stresses were calculated from the strain distribution $\varepsilon_{\varphi\psi}\{hkl\}$ derived from the measured inter-reticular plane spacing and the elastic radio crystallographic constants, $S_1\{hkl\}$ and $½S_2\{hkl\}$, which are equal to -3.13×10^{-6} MPa^{-1} and 11.79×10^{-6} MPa, respectively, for OFHC copper. X-ray Mn-Kα radiation (18 kV at 4 mA) was used to determine the elastic strains in the (311) planes (149.09° Bragg angle). Residual stresses were determined in the machined surface and subsurface, in the cutting direction and parallel to the cutting edge.

To evaluate the dislocation density and the crystalline domain size, a measurement of the Bragg peak broadening of the dislocation/defect density in the diffracting domain was performed using X-ray diffraction. In fact, for a simple Gaussian distribution, the full width at half maximum (FWHM) may be related to the dislocation density (ρ) and the crystalline domain size (d_{crys}) when the model of Williamson and Smallmann [13] is used.

Grain size measurements were performed using an optical microscope (OLYMPUS BX51M) after electropolishing (Struers LectroPol-5) the surfaces with phosphoric acid to reveal the grain boundaries. Vickers microhardness (*HV*) was also measured on each specimen using a microhardness tester (TUKONTM1202, Wilson Hardness), applying a load of 25 g according to *EN ISO* 6507-1.

2.3. Electrochemical microcell tests

The object of the tests was to investigate the effects of varying the cutting parameters on polarization curves. These curves show essentially the current density inside the cathodic domain (I_{cath}), the current density in the passive plate (I_{pass}) consisting of the steady state anodic current density which serves as a measure of the average dissolution rate at a given potential, and the pitting potential (E_b).

The local electrochemical behavior of specimens was studied in 1 M $NaClO_4$ solution at a room temperature of 25 °C using the electrochemical microcell technique. This technique uses a glass microcapillary that is filled with electrolyte (Figure 2). The microcapillary tip was sealed to the specimen surface with a layer of silicon rubber. The microcell was mounted on a microscope for precise positioning of the microcapillary on the surface. The diameter of the microcapillary tip was 50 µm. The counter electrode was a platinum wire, and the reference electrode was Ag/AgCl. A modified high-resolution potentiostat was used for a current detection of approximately 20 fA. The potentiodynamic polarization curves were determined from −600 mV vs. Ag/AgCl to the anodic direction at the potential scan rates (1 mV s^{-1}). The current was low-pass filtered and the cutoff frequency was 20 Hz. Reactions taking place during copper corrosion under the saline solution of NaCl can be explained by the description given in the reference [14].

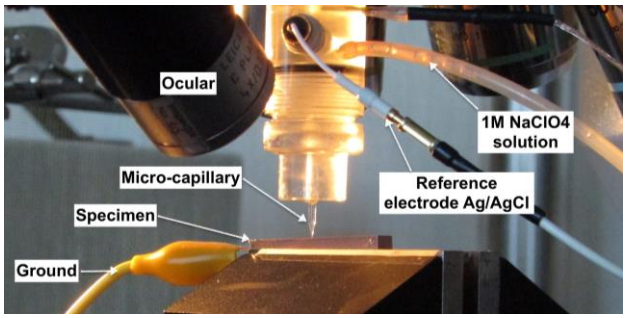

Figure 2. *Disposition of the specimen, the microcapillary and the electrodes for the micro-cell electrochemical analysis.*

3. Experimental results

3.1. Observations

The potentiodynamic polarization measurements (Figure 4) showed that the electrochemical behavior of OFHC copper surfaces is very sensitive to the cutting conditions in terms of cutting speed, uncut chip thickness, or tool geometry. However, during the cutting process, simple observations cannot establish the corresponding relationships, therefore statistical analysis must be used to reveal those relations. In fact, the polarization curves obtained by each tested surface (Figure 4) are used to extract the current density in the cathodic domain I_{cath} (Figure 3a), the current density in the passive plate I_{pass} (Figure 3b), and the pitting potential E_b (Figure 3c). Classifying the resulting values from the highest to the lowest has shown some relationships: the highest I_{cath} and I_{pass} values are obtained for the highest cutting speed (V_c = 120 m/min) used in all cases (Figure 3a and Figure 3b), but the highest pitting

potential E_b is obtained for the lowest uncut chip thicknesses h (Figure 3c) with the exception of two cases, ($\gamma = 20°$, $\alpha = 5°$, $h = 0.2$ mm, and $V_c = 120$ m/min) and ($\gamma = 30°$, $\alpha = 5°$, $h = 0.05$ mm, and $V_c = 90$ m/min), which can be because of a possible synergy effect between h and another cutting condition.

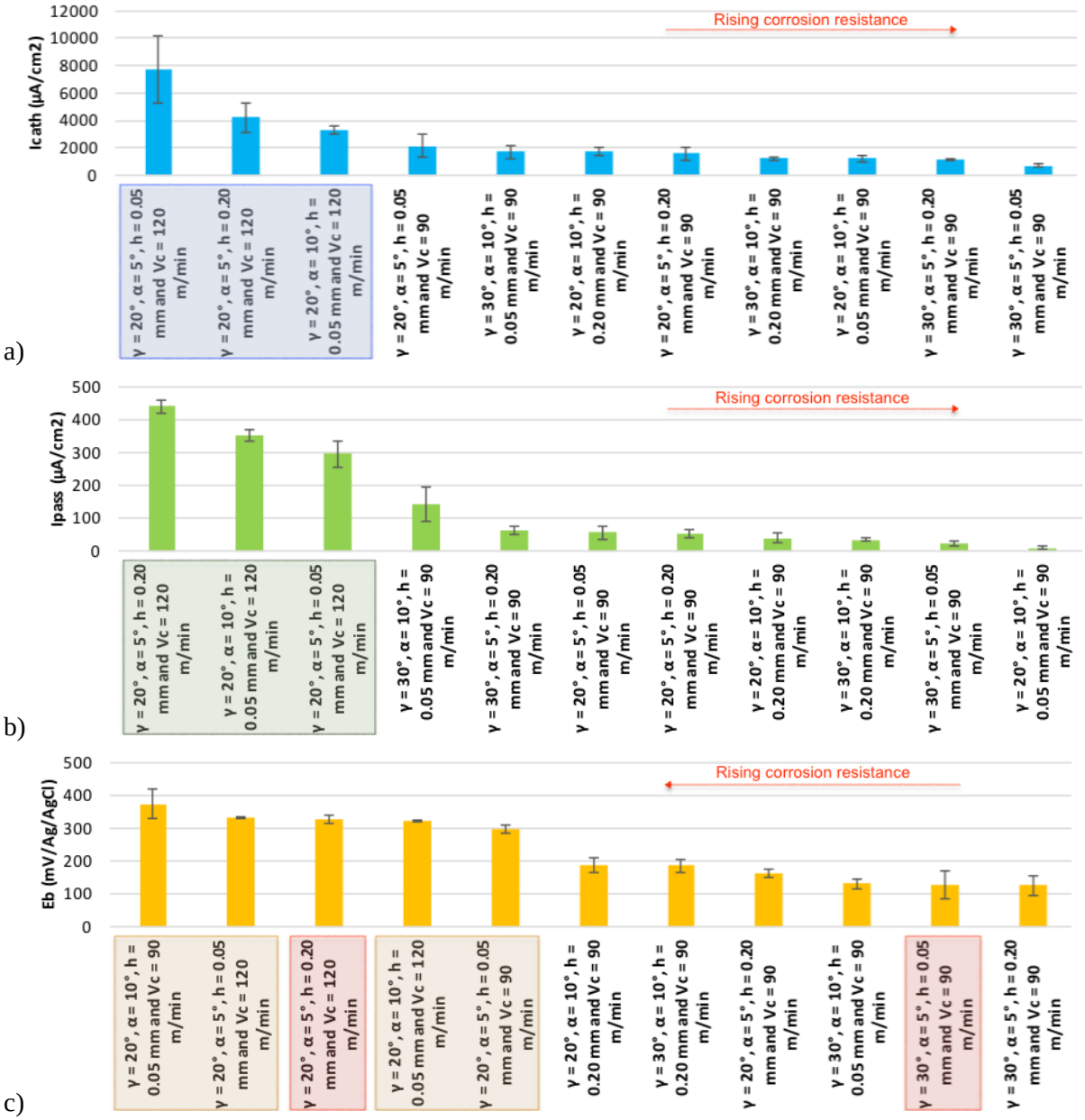

Figure 3. *Impact of the cutting conditions variation on: (a) the current density in the cathodic domain I_{cath}; (b) the current density in the passive domain I_{pass}; and (c) the pitting potential E_b.*

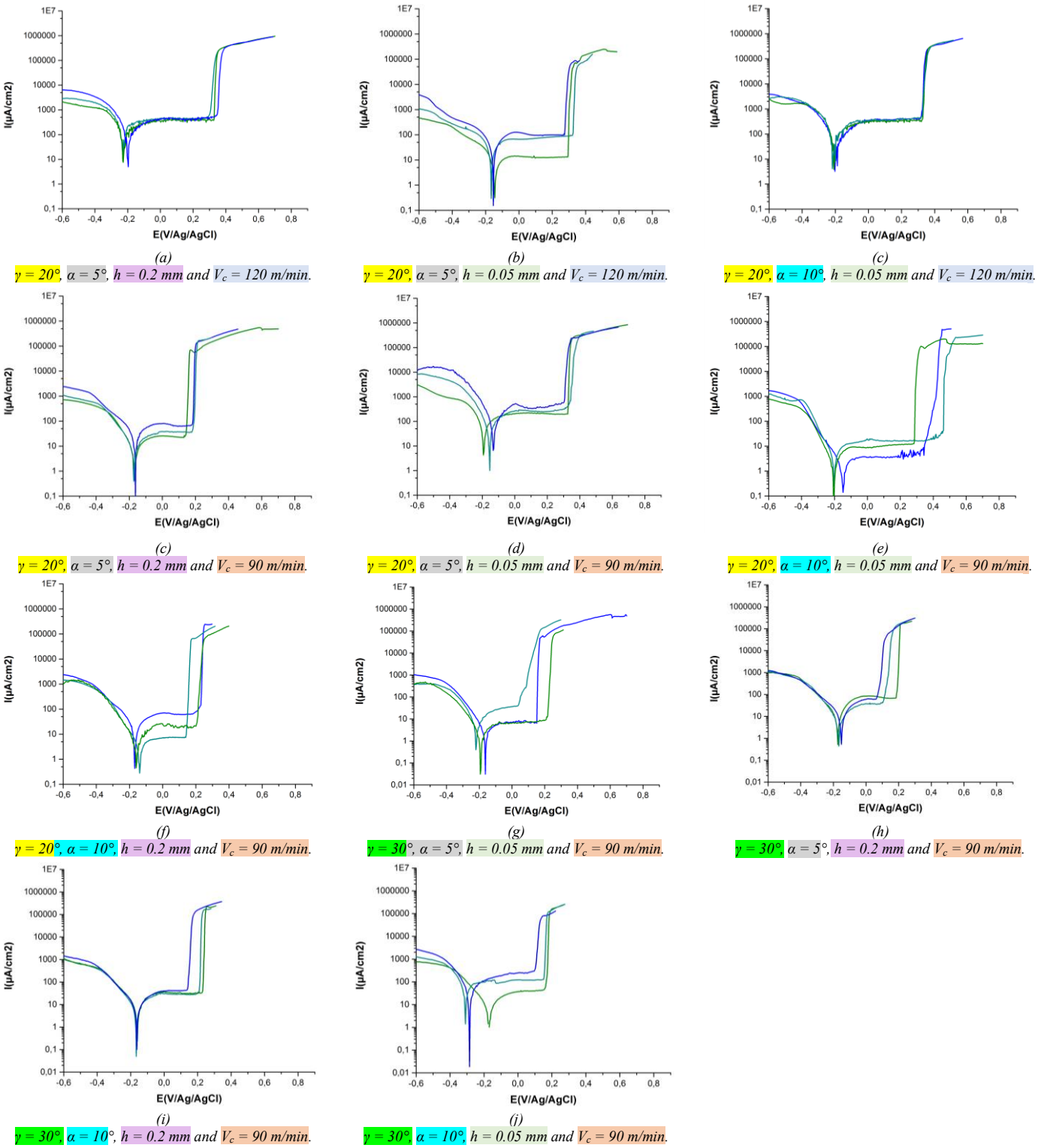

(a) $\gamma = 20°$, $\alpha = 5°$, $h = 0.2$ mm and $V_c = 120$ m/min.

(b) $\gamma = 20°$, $\alpha = 5°$, $h = 0.05$ mm and $V_c = 120$ m/min.

(c) $\gamma = 20°$, $\alpha = 10°$, $h = 0.05$ mm and $V_c = 120$ m/min.

(c) $\gamma = 20°$, $\alpha = 5°$, $h = 0.2$ mm and $V_c = 90$ m/min.

(d) $\gamma = 20°$, $\alpha = 5°$, $h = 0.05$ mm and $V_c = 90$ m/min.

(e) $\gamma = 20°$, $\alpha = 10°$, $h = 0.05$ mm and $V_c = 90$ m/min.

(f) $\gamma = 20°$, $\alpha = 10°$, $h = 0.2$ mm and $V_c = 90$ m/min.

(g) $\gamma = 30°$, $\alpha = 5°$, $h = 0.05$ mm and $V_c = 90$ m/min.

(h) $\gamma = 30°$, $\alpha = 5°$, $h = 0.2$ mm and $V_c = 90$ m/min.

(i) $\gamma = 30°$, $\alpha = 10°$, $h = 0.2$ mm and $V_c = 90$ m/min.

(j) $\gamma = 30°$, $\alpha = 10°$, $h = 0.05$ mm and $V_c = 90$ m/min.

Figure 4. *Polarization curves obtained by analyzing surfaces of OFHC copper machined by orthogonal cutting process.*

3.2. Statistical analysis

In this section, all results concerning surface integrity and local electrochemical behavior are treated using a statistical approach to identify the surface integrity parameters that have relevant impact on

electrochemical behavior of the surfaces. Then, for those parameters identified as relevant, the cutting conditions affecting them are also identified.

For results analysis, two statistical treatments are performed: the Bravais-Pearson correlation analysis and the analysis of variance (ANOVA). The statistical approach is explained in Figure 5.

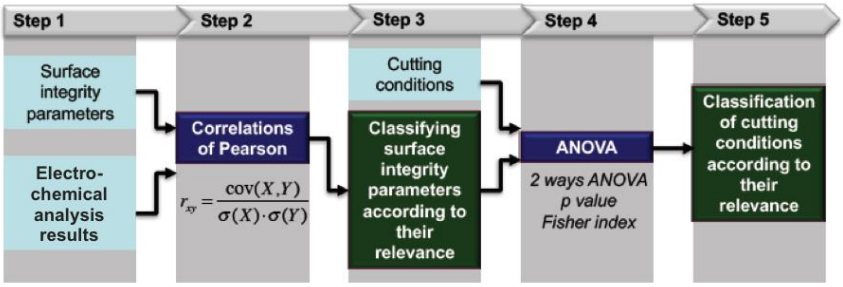

Figure 5. *Multi-physical analysis approach.*

The first step consists in gathering all the experimental and numerical measured values concerning electrochemical behavior (Table 1) and surface integrity (Table 2) in the order of the cutting conditions used, given by Table 3.

Table 1. *Results issued from local electrochemical analysis.*

Test N°	I_{cath} µA/cm²	I_{pass} µA/cm²	E_b mV/Ag/AgCl	eI_{cath} µA/cm²	eI_{pass} µA/cm²	eE_b mV/Ag/AgCl
1	7684	294	331	4823	79	9
2	3263	351	322	563	34	3
3	4220	438	325	2188	43	24
4	1559	53	162	843	28	23
5	1718	141	131	960	102	29
6	2140	55	297	1680	42	26
7	1230	35	185	202	7	43
8	1702	39	185	607	32	46
9	1088	61	125	112	23	59
10	706	21	127	309	14	89
11	1203	10	372	455	6	90

Table 2. *Results issued from experimental and numerical analysis of the surface integrity.*

Test N°	σ_x MPa	σ_y MPa	Plastic layer thickness µm	S_a nm	S_t µm	d_{grain} µm	d_{crys} nm	ρ µm/µm³	Microhardness $HV_{0.025}$
1	228	145	61	471	22.6	9.7	27	1230	122
2	188	148	214	493	5.6	10	25	1420	122
3	137	116	777	495	18.1	8.2	38	617	128
4	106	81	678	626	17.4	7.7	167	32	130
5	134	118	195	672	31	14	29	1080	114
6	181	145	44	471	22.6	5.4	27	1260	146
7	59	50	362	662	15.3	6.1	47	425	139
8	-10	9	794	677	16.9	7.1	180	29	134
9	36	41	384	461	20.9	5.2	52	355	148
10	204	105	151	440	18.8	3.1	26	1320	186
11	206	130	149	550	5.7	8	99	92	128

Table 3. *Cutting conditions while orthogonal cutting.*

Test N°	γ °	α °	h mm	V_c m/min
1	20	5	0.05	120
2	20	10	0.05	120
3	20	5	0.2	120
4	20	5	0.2	90
5	30	10	0.05	90
6	20	5	0.05	90
7	30	10	0.2	90
8	20	10	0.2	90
9	30	5	0.2	90
10	30	5	0.05	90
11	20	10	0.05	90

The second step consists in calculating Bravais-Pearson's correlations for each pair (surface integrity parameter/electrochemical parameter). The correlation coefficient r_{xy} is calculated as follows:

$$r_{xy} = \frac{\mathrm{cov}(X,Y)}{\sigma(X)\cdot\sigma(Y)} \quad \textbf{(1)}$$

with σ the standard deviation and $cov(X,Y)$ the covariance of the variables X and Y. In this study, the variable X corresponds to a parameter extracted from the polarization curves (I_{cath}, eI_{cath}, I_{pass}, eI_{pass}, E_b, and eE_b). The variable Y corresponds to a surface integrity parameter (Surface residual stress measured in the cutting direction σ_x, surface residual stress measured in the transversal direction σ_y, plastic layer thickness, surface arithmetic roughness S_a, surface roughness at maximum height S_t, grains size on the surface d_{grain}, dislocations density on the surface ρ, and microhardness HV). The value of the correlation coefficient is normalized, defined between -1 and 1. This coefficient is used to characterize a linear

positive or negative relationship. The closer it is to 1 (evaluated in absolute value), the stronger the relationship. A null r_{xy} indicates the absence of any correlation.

The third step consists in identifying surface integrity parameters having significant Pearson correlation coefficients. As deviations of the estimated parameters are considered theoretically possible in either direction from some benchmark value, a two-tailed probability test is performed. For a two-tailed probability with 9 degrees of freedom *df* (*df* = number of trials - 2), the significance threshold is 0.5 corresponding to a test performed at a 10% level (a *p-value* less than 0.1), i.e., there is a maximum of 10% chance of wrongly rejecting the null hypothesis supposing the absence of any relationship between the two tested sets. Correlation analysis permitted the identification of the influent parameters regarding electrochemical behavior, i.e., having $r_{xy} \geq 0.5$ (Figure 6a and Figure 6b).

a)

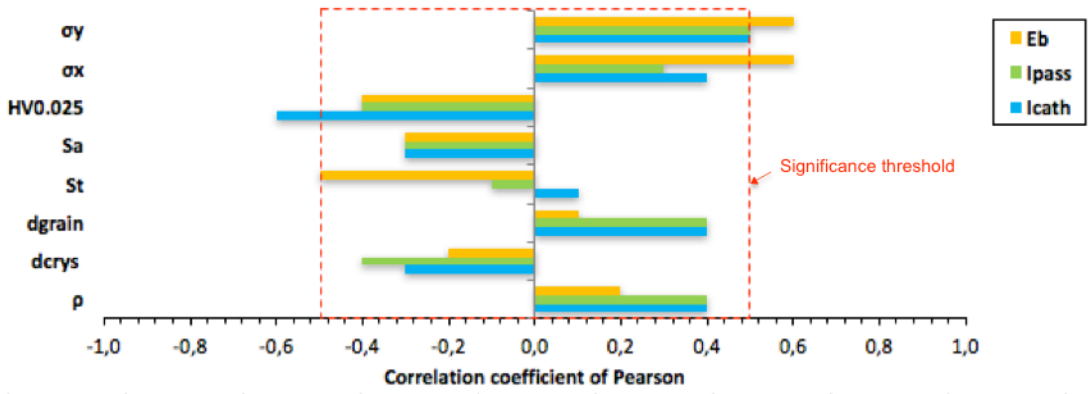

b)

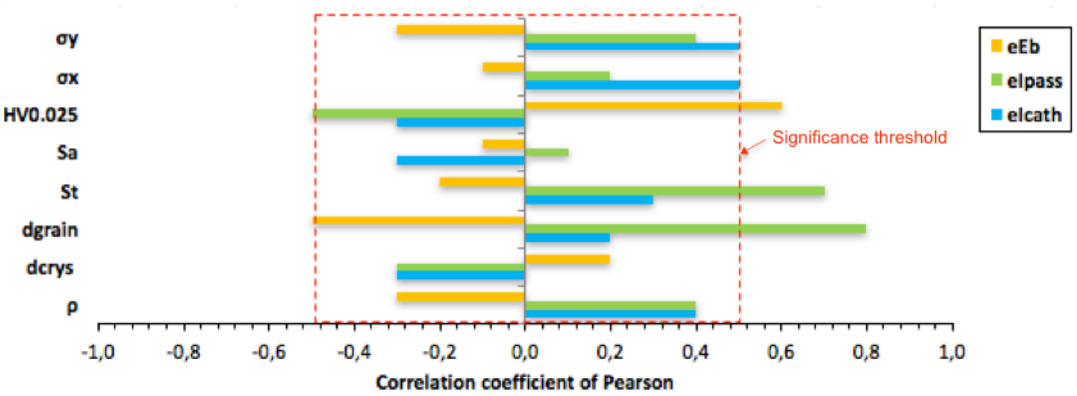

Figure 6. *Pearson's correlation coefficients concerning the parameters of: (a) local electrochemical behavior and (b) their corresponding dispersions of measurements.*

Concerning the local electrochemical behavior and the parameters obtained from polarization curves, it is clear that only the residual stress σ_y and the microhardness *HV* significantly influence the current density in the cathodic domain I_{cath} (Figure 6a), aside from the deviation of the measured values (reflecting the repeatability of the process) eI_{cath} (Figure 6b). Concerning the passivation of the surface, only the residual stress σ_y seems to significantly influence I_{pass} (Figure 6a). However, the repeatability of the measurement eI_{pass} depends firstly on the grain size d_{grain}, then on the roughness at maximal profile

height S_t (Figure 6b). Finally, for local pitting corrosion, it has been shown that the pitting potential E_b depends in a first order on the residual stresses σ_x then σ_y, and in a second order on the roughness S_t (Figure 6a). Nevertheless, its dispersion depends on the microhardness and the grain size d_{grain} (Figure 6b). Those results are summarized in Table 4.

Table 4. *Ranking of the parameters influencing the electrochemical behavior of the machined surfaces.*

Electrochemical behavior	Parameters of surface integrity significantly relevant		
	1st parameter	**2nd parameter**	**3rd parameter**
E_b	Residual stress σ_y	Residual stress σ_x	Roughness at maximum height S_t
eE_b	Microhardness HV	(-) Grain size d_{grain}	
I_{pass}	Residual stress σ_y		
eI_{pass}	Grain size d_{grain}	(-) Roughness at maximum height S_t	(-) Microhardness HV
I_{cath}	Residual stress σ_y	(-) Microhardness HV	
eI_{cath}	Residual stress σ_y	Residual stress σ_x	

**(-) means inversely correlated to the corresponding electrochemical parameter*

In the fourth step, the selected parameters become the object of the two-way ANOVA as functions of the cutting conditions, and their double interactions for synergy effects are revealed. Indeed, Fisher index values are calculated, and those higher than 2 are considered of relevance, as the corresponding dissociation probabilities (*p*-values*)* are lower than 0.1. All calculations are carried out using the software Minitab Express.

In the fifth step, according to Fisher index values (Table 5), every relevant surface integrity parameter is associated to the corresponding cutting conditions.

Table 5. *Fisher index values.*

	γ	**α**	**h**	**V_c**	**V_c×h**	**V_c×α**	**h×α**	**h×γ**	**α×γ**
S_t	1.8	1.4	0.0	0.4	0.3	1.4	0.2	1.2	3.8
d_{grain}	0.2	2.2	0.7	1.3	0.0	0.4	2.5	0.3	2.6
HV	2.1	2.0	0.0	1.7	0.2	0.7	1.9	0.1	4.3
σ_x	0.6	0.5	20.6	1.9	1.2	0.1	0.7	0.0	0.0
σ_y	1.2	0.2	15.8	3.1	2.4	0.3	2.3	0.0	0.3

After the two-way ANOVA between the identified parameters and the cutting conditions was run to identify their interactions, the Fisher index analysis gave the following result according to the order of influence on surface integrity (Table 6):

1- The uncut chip thickness h is a first-order parameter having the highest impact on the residual stresses (F_i = 20.6 for σ_x and 15.8 for σ_y).

2- The interaction flank angle with rake angle ($\alpha \times \gamma$) is a second-order parameter having the highest impact on the microhardness, the roughness, and the grain size ($F_i = 4.3$ for HV, 3.8 for S_t and 2.6 for d_{grain}).

3- The cutting speed (V_c) is a second-order parameter having a significant impact on the residual stress in the cutting direction ($F_i = 3.1$ for σ_y).

Table 6. *Cutting conditions influencing the relevant surface integrity parameters.*

Surface integrity parameter	Cutting conditions and synergy effects significantly influent		
	1st order	2nd order	3rd order
Residual stress σ_y	(-) Uncut chip thickness h	Cutting speed V_c	$V_c \times h$; $h \times \alpha$
Residual stress σ_x	(-) Uncut chip thickness h		
Microhardness HV			Rake angle γ; Flank angle α
Grain size d_{grain}			$\alpha \times \gamma$; $h \times \alpha$; Flank angle α
Roughness at maximum height S_t		$\alpha \times \gamma$	

Finally, the connection between the electrochemical behavior, the surface integrity, and the cutting parameters for the particular case of OFHC copper surfaces obtained by orthogonal cutting can be illustrated as shown in Figure 7:

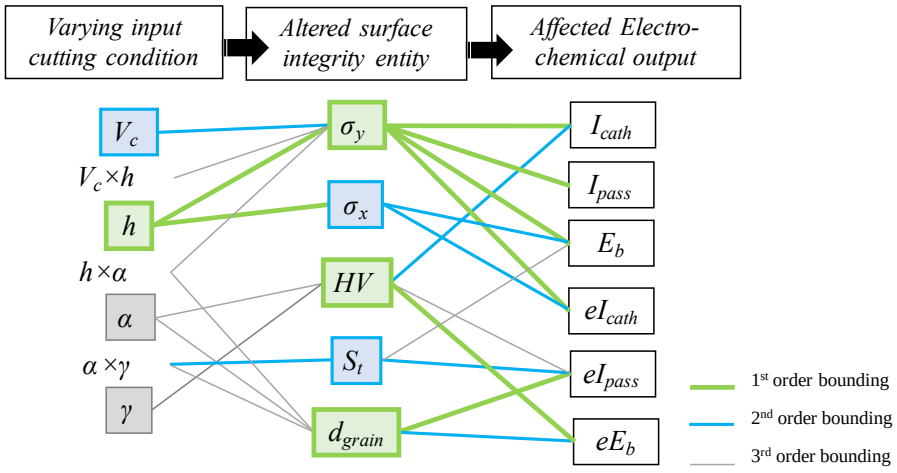

Figure 7. *Bounding between the electrochemical behavior parameters, surface integrity and cutting conditions for OFHC copper orthogonal cutting.*

Although relationships between the different parameters studied were identified, the physical origins of those links should be clarified; these are discussed in the next section.

4. Discussion

The statistical analysis has highlighted the impact of machining on surface integrity, which has been shown to affect corrosion resistance. A physical explanation of the revealed relationship follows in Section 4.1.

4.1. Impact of the surface integrity on the electrochemical behavior

For instance, the influence of the passive film formation on the anodic and cathodic reactions is important, as copper and copper alloys are generally only viable as corrosion-resistant materials in the 'passive' state [1]. At such filmed or blocked surfaces, transport processes occurring through poorly conducting solid corrosion product layers limit both the overall anodic and the cathodic reaction rates.

The amplitude of the residual stresses affects the free energy of the material that, in return, has an impact on the work function of the electrons on the surface [15]. The residual stresses are shown as the first-order parameters influencing the local electrochemical behavior. In fact, the common action of corrosion and the tensile residual stress results in this corrosion phenomenon appearing on the surface. Being passive, its protecting oxide film is locally broken under the action of tensile stresses, creating vacancies in the film [16]. The conductivity of the passive film increases, leading to local corrosion. For that reason, increasing tensile residual stresses accelerates the anodic reaction (dissolution of the surface). However, considering their impact on microhardness, it has been proven that residual stresses and microhardness are related to each other, and even linear relationships can be found for the case of copper and copper alloys [17]. For that reason, the high correlation found between microhardness and electrochemical behavior is a consequence of the effect of residual stresses. Moreover, it is natural that the residual stress appears as a factor highly correlated to the electrochemical behavior of the surfaces, as pitting corrosion resistance of the samples is diminished with increased mechanical load, presumably because of the increase in the defect density [18].

The microstructure grain size has an important impact on the electrochemical behavior of the machined surface. In fact, it affects the energy of formation of the charged defaults during the thickening of the passive film, and influences the exchanges inside the oxide film. In literature, it has been demonstrated that a high density of grain boundaries promotes the formation of the passive film as the electrons are more active at the boundaries [15]. Moreover, in some conditions, grain boundaries are the locations of a high degree of localized corrosion while the remaining material is intact (intergranular corrosion). However, the dispersions seen in the measurement of the pitting potential can be explained by the heterogeneity of the machined surface microstructure at the local scale. In fact, it is worth noting that the measured grain size is an average value, and a local electrochemical analysis (possibly performed on an area containing a majority of small grains) will not give the same electrochemical response as an analysis performed on an area containing a mixture of big and small grains with an equal average grain size. In that case, the value of the anodic current is determined largely by the grain boundary state and depends on the heat loading applied to the initial material; the corrosion properties degrade and the average dissolution rate increases with the presence of ultra-fine grains [19].

Moreover, according to the statistical analysis, the surface roughness at maximum height S_t is a parameter having a substantial influence on the electrochemical reactivity of the surfaces. Many

hypotheses can be proposed to explain this correlation. In fact, it is demonstrated that the roughness affects the electronic behavior, described by the *EWF* of copper. The local fluctuation of the *EWF* increases with the increase of the roughness [10]. Such fluctuation favors the formation of microelectrodes, and as a result, accelerates corrosion. Furthermore, the density of the local charges can increase with the increase of the local roughness. Such an heterogeneous distribution of the charges density promotes the initiation of pitting [20].

4.2. Impact of cutting conditions on surface integrity

The longitudinal residual stress measured on the surface in the cutting direction σ_x is associated with the uncut chip thickness h (it diminishes with the increase of h). However, the residual stress in the transverse direction parallel to the cutting edge σ_y is not only associated with the uncut chip thickness h (also diminishing with the increase of h) but also with the cutting speed V_c (increases with V_c), in addition to their interactions $V_c \times h$ (synergy effect) and $h \times \alpha$. In fact, residual stresses are the result of mechanical and thermal charges taking place around the cutting edge. Starting from that point, two hypotheses are to be verified to explain the obtained observations: the influence of temperature distribution and the influence of the state of stress; in particular, the stresses' triaxiality. The impact of h and V_c on the distribution of the cutting temperatures can be checked using numerical simulation [21]. However, the temperature increase in the machined surface induced by cutting is low, and the yield stress varies only about 1.7%. As the temperature variation from one cutting condition to another one is still not significant, residual stresses are then essentially generated by mechanical loadings induced by the tool/material contact. According to Denguir et al. [21], the falling triaxiality η occurring at the chip root implies an increase of the equivalent strain, ε_f, at damage initiation. Consequently, the residual stress σ_R is found to be more tensile. In fact, it has been demonstrated that an increase occurs in the triaxiality when the cutting speed V_c decreases in the deformation zone. Moreover, a clear increase in triaxiality occurs while increasing the uncut chip thickness h, more precisely, at the separation point of the chip from the workpiece. That implies a decrease of the strain at damage initiation ε_f of the workmaterial. This induces a decrease of the cutting energy and consequently, the residual stresses are decreased.

The grain size is associated with the interaction ($\gamma \times \alpha$), then ($h \times \alpha$), and finally with less relevance, to the angle α. In fact, as shown in Figure 8, grain sizes in the surface are altered by the change in the cutting conditions. Grains can break or be elongated and deformed according to a privileged direction (making an inclination angle with respect to the cutting direction) under mechanical loading (the cutting forces). The mechanical loading increases with the increase of the uncut chip thickness h, the reduction of the rake angle γ, or adhesion phenomena that can occur with small flank angles α [22-25].

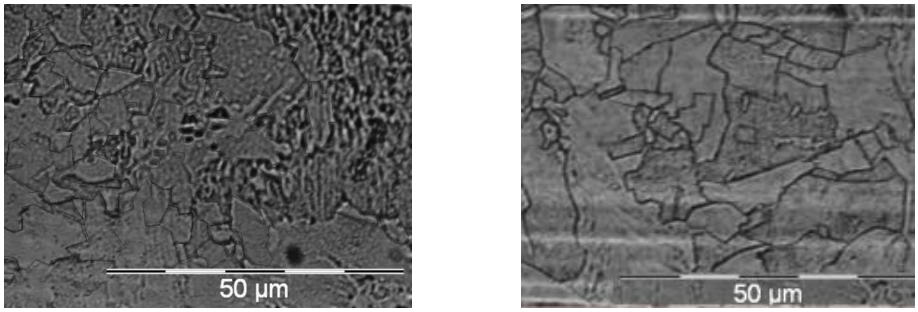

(a) *(b)*

Figure 8. *Microstructure of the surfaces obtained by optical microscopy issued from the cutting conditions (a) $\gamma = 30°$, $\alpha = 10°$, $h = 0.2$ mm and $V_c = 90$ m/min and (b) $\gamma = 30°$, $\alpha = 10°$, $h = 0.05$ mm and $V_c = 90$ m/min* [21].

The surface roughness at maximum height S_t is found to be associated with the cutting tool geometry, in particular with the interaction ($\gamma \times \alpha$). Characterizing the maximum height profile, and in absence of machining striae created by the tool geometry, it reflects the existence of micro tearing and adhesion of the material on the generated surface. In fact, in the case of orthogonal cutting, roughness is related to the profile of the cutting edge (tool wear is not taken into account in this study, as all trials were performed with new tools), but it is essentially related to the tool edge geometry defaults and to the adhesive friction between the flank face and the surface of the workpiece, frequently seen in the case of ductile materials (e.g., annealed copper, the work material) when it is machined with small relative cutting edges inducing micro tearing [23]. It is exactly the case observed while machining copper (Figure 9). Adhesion and micro-tearing occur because of the ratio between the shear stress and the normal stress inside the zone adjacent to the cutting edge radius at the contact tool/workpiece (flank contact) approaching or exceeding 1, creating conditions that favor adhesion [24]. Therefore, a small rake angle raises the shear stress in this zone; when associated with a small flank angle, they induce adhesion.

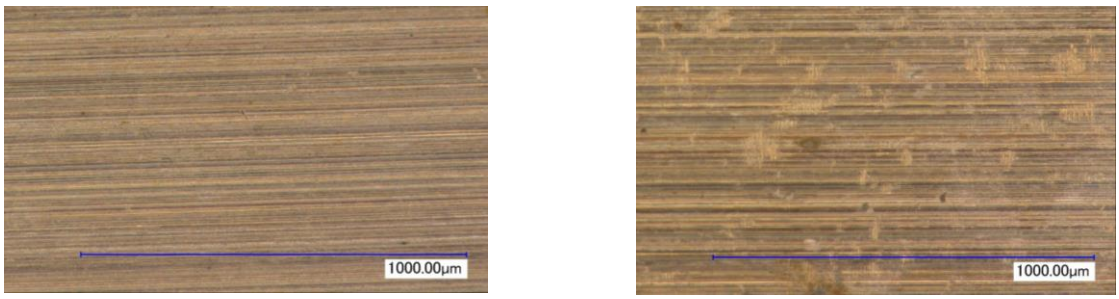

(a) *(b)*

Figure 9. *(a) Surface machined using $\gamma = 20°$, $\alpha = 10°$, $h = 0.05$ mm and $V_c = 120$ m/min ; (b) Micro tearing in the case of $\gamma = 20°$, $\alpha = 5°$, $h = 0.05$ mm and $V_c = 120$ m/min.*

5. Conclusion

A statistical multi-physical analysis using the correlations of Pearson and the two-way ANOVA as techniques is applied to the results obtained from the cutting operations, the surface integrity, and the electrochemical analysis of the surfaces obtained by orthogonal cutting of OFHC copper. Physical explanations of the observed phenomena are given.

The results expose a significant influence of the surface integrity on the material dissolution and the risk of corrosion. Then, it is proven that an increase of the tensile residual stresses can accelerate the anodic reaction (dissolution of the surface) highlighting the risk of developing pitting corrosion. Moreover, a rough surface is more susceptible to developing dissolution, as the micro peaks can function as microelectrodes. Nevertheless, grain refinement at the surface and the increase in hardness favor metal passivation and delay the risk of pitting. Making the link with the cutting conditions, for a better corrosion resistance of OFHC copper surfaces obtained by finishing machining, it is recommended to maximize both the thickness of cut h and the cutting speed V_c, leading to a reduction in the tensile residual stresses at the surface, which are implicated in promoting the breakage of the passive film of oxide that protects the copper.

However, concerning to the rake angle γ, contrary to what is usually recommended for ductile materials machining to minimize cutting energy, the reduction of the rake angle can be beneficial for the sustainability of the machined surface. In fact, a lower rake angle leads to a higher surface hardness and smaller grain size, which complicates the development of the dissolution process. Therefore, with low rake angles, it is recommended to avoid low flank angles α in order to minimize adhesive friction in the flank face leading to micro tearing, which leads to favorable sites for dissolution initiation.

Acknowledgments

The authors acknowledge the technical and financial support of CEA Valduc (21120 Is sur Tille, France) and their laboratory LIMPE (Interaction Matériau-Procédé-Environnement, LRC DAM-VA-11-02, France). They also thank Pr. V. Vignal for his guidance, his valuable remarks and for hosting the corrosion tests in his laboratory ICB UMR 6303 (France).

Declaration of Competing Interests

The authors have no competing interests to declare.

References

[1] G. Kear, B. Barker, and F. Walsh, “Electrochemical corrosion of unalloyed copper in chloride media — a critical review,” *Corrosion Science*, vol. 46, pp. 109–135, 2004. https://doi.org/10.1016/S0010-938X(02)00257-3

[2] P. Fernandez-Zelaia and S. N. Melkote, "Analysis of structure-property gradients in orthogonally machined chips and workpiece subsurface," *CIRP Annals*, vol. 69, issue 1, pp. 89-92, 2020.

https://doi.org/10.1016/j.cirp.2020.04.020
[3] N. Mary, V. Vignal, R. Oltra, and L. Coudreuse, “Finite-element and XRD methods for the determination of the residual surface stress field and the elastic–plastic behaviour of duplex steels,” *Philosophical Magazine*, vol. 85, pp. 1227–1242, 2005.
https://doi.org/10.1080/14786430412331333329
[4] V. Vignal, N. Mary, R. Oltra, and J. Peultier, “A Mechanical–Electrochemical Approach for the Determination of Precursor Sites for Pitting Corrosion at the Microscale,” *Journal of The Electrochemical Society*, vol. 153, no. 9, p. B352, 2006.
https://doi.org/10.1149%2F1.2218762
[5] V. Vignal and D. Kempf, “Influence of Heterogeneous Plastic Strain Fields on the Corrosion Susceptibility of Duplex Stainless Steels at the Microscale,” *Advances In Materials Science*, vol. 7, no. 11, pp. 77–82, 2007.
Identyfikator YADDA: bwmeta1.element.baztech-article-BPG5-0025-0010
[6] H. Krawiec, V. Vignal, and J. Banas, “Macroscopic and Local Electrochemical Studies of Austempered Ductile Iron in Perchlorate Solutions,” *Journal of The Electrochemical Society*, vol. 153, no. 7, p. B231, 2006.
https://doi.org/10.1149/1.2197635
[7] H. Krawiec, V. Vignal, and Z. Szklarz, “Local electrochemical studies of the microstructural corrosion of AlCu4Mg1 as-cast aluminum alloy and influence of applied strain,” *Journal of Solid State Electrochemistry*, vol. 13, no. 8, pp. 1181–1191, Aug. 2009.
https://doi.org/10.1007/s10008-008-0638-8
[8] S. Bissey-Breton, J. Farré, V. Vignal, N. Mary, and N. Mary, “Impact des conditions d’usinage sur la zone du matériau affectée par le procédé,” *Mécanique & Industries*, vol. 8, no. 3, pp. 193–197, May 2007.
https://doi.org/10.1051/meca:2007038
[9] S. Bissey-Breton, J. Gravier, and V. Vignal, “Impact of superfinish turning on surface integrity of pure copper,” *Procedia Engineering*, 2011, vol. 19, pp. 28–33.
https://doi.org/10.1016/j.proeng.2011.11.075
[10] W. Li and D. Y. Li, “Influence of surface morphology on corrosion and electronic behavior,” *Acta Materialia*, vol. 54, no. 2, pp. 445–452, 2006.
https://doi.org/10.1016/j.actamat.2005.09.017
[11] S. Yin and D. Y. Li, “Effects of prior cold work on corrosion and corrosive wear of copper in HNO3 and NaCl solutions,” *Materials Science and Engineering A*, vol. 394, no. 1–2, pp. 266–276, 2005.
https://doi.org/10.1016/j.msea.2004.11.054
[12] L. Denguir, J. Outeiro, G. Fromentin, V. Vignal, and R. Besnard, “Influence of cutting process mechanics on surface integrity and electrochemical behavior of OFHC copper,” *Procedia CIRP*, 2014, vol. 13.
https://doi.org/10.1016/j.procir.2014.04.032
[13] G. K. Williamson and R. E. Smallmann, “Dislocation densities in some annealed and cold-worked metals from measurements on the X-ray Debye-Scherrer spectrum,” *Philosophical Magazine*, vol. 1, no. 1, pp. 34–46, 1956.
https://doi.org/10.1080/14786435608238074
[14] J. Gravier, V. Vignal, and S. Bissey-Breton, “Influence of residual stress, surface roughness and crystallographic texture induced by machining on the corrosion behaviour of copper in salt-fog atmosphere,” *Corrosion Science*, vol. 61, pp. 162–170, 2012.
https://doi.org/10.1016/j.corsci.2012.04.032
[15] K. D. Ralston and N. Birbilis, “Effect of grain size on corrosion: A Review,” *Corrosion*, vol. 66, no. 7, p. 75005, 2010.
https://doi.org/10.5006/1.3462912
[16] V. Vignal, C. Valot, R. Oltra, M. Verneau, and L. Coudreuse, “Analogy between the effects of a mechanical and chemical perturbation on the conductivity of passive films,” *Corrosion Science*, vol. 44, pp. 1477–1496, 2002.
https://doi.org/10.1016/S0010-938X(01)00162-7
[17] S. C. Krishna, N. K. Gangwar, A. K. Jha, and B. Pant, “On the Prediction of Strength from